

## Threshold energy estimates of TACTIC gamma-ray telescope array — Inputs from simulation studies (I)

N. Sathyabama, M. L. Sapru, C. L. Bhat, R. C. Rannot, A. K. Razdan,  
A. K. Tickoo, M. K. Koul and V. N. Gandhi

*Bhabha Atomic Research Centre, Nuclear Research Laboratory, Mumbai 400085, India*

**Abstract.** Comprehensive simulation studies, using the CORSIKA air-shower code are in progress to predict and optimize the performance of the TACTIC  $\gamma$ -ray telescope array. Preliminary results are presented here on the  $\gamma$ -ray threshold energies likely to be achieved by its Central Imaging Element and 3 Vertex Elements, using 2 independent, innovative trigger-generation criteria.

### 1. Introduction

The  $\gamma$ -ray telescope TACTIC, presently in the installation phase in the Western Indian hill-station of Mt. Abu, Rajasthan ( $24^{\circ}.6$  N,  $72^{\circ}.7$  E, 1300 m asl), in an array of 4 atmospheric Cerenkov telescopes with each telescope element having a light collector composed of  $32 \times 0.6$ m-diameter spherical mirrors of  $\sim 4$ m focal length (Bhat, 1996). The 4 elements of the array are disposed in a triangular configuration, with 3 elements at the vertices (VE) and an imaging element (IE) at the centroid of a triangle of side 20m (Fig. 1a). A hybrid approach

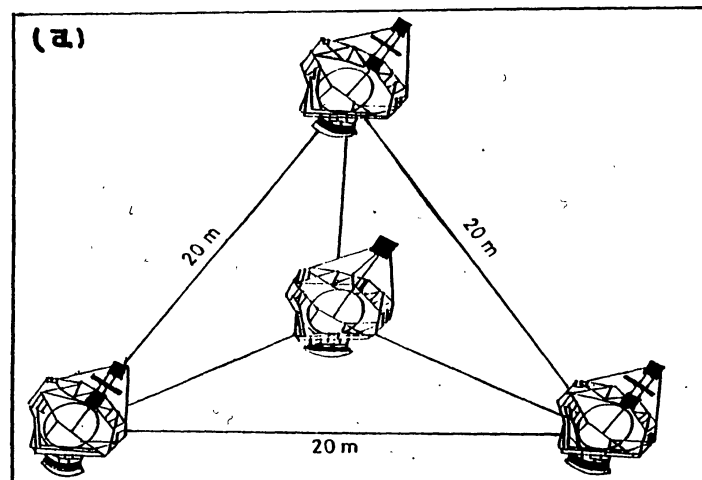
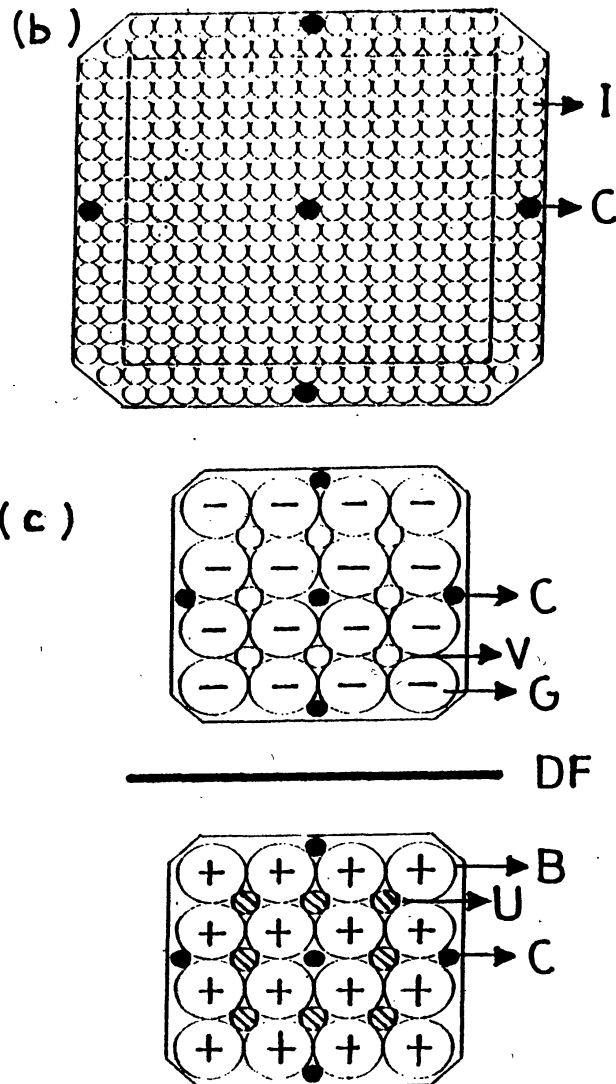


Figure 1(a). A block-diagram of the TACTIC array, presently, under installation at Mt. Abu.

is followed for the TACTIC focal-plane instrumentation (Fig. 1b and 1c), with the IE using a high-definition Cerenkov imaging camera comprising 349 photomultiplier pixels (matrix configuration :  $19 \times 19$ , FOV : 6, pixel resolution :  $0.31^\circ$ ) and the VE deploying non-imaging, photomultiplier-based arrays (FOV :  $3.6^\circ$ , pixel sizes  $0.9^\circ$  and  $0.31^\circ$ ; for more details see Bhat, 1996). The IE event trigger is being derived from the central  $15 \times 15$  pixels of the camera, using a novel proximity trigger-generation strategy, called 3NCT for Nearest-Neighbour Non-Collinear Triplet triggers (Bhat et al., 1994). In the case of VE, the main emphasis is on seeking a higher flux sensitivity by operating these elements at a significantly Lower Threshold than what is practical in the case of IE — the LT-mode of VE operation, especially suitable for pulsar searches (Vishwanath, 1996). This novel mode of operation (Bhat et al., 1995)



**Figure 1(b).** Front-end instrumentation of the TACTIC imaging element. (c): 3 Vertex Elements. B : Blue, G : Green pixels ( $\Delta\theta = 0.9^\circ$ ), I : Image, C : Calibration, V : Visible, U : Ultraviolet pixels ( $\Delta\theta = 0.31^\circ$ ); DF : Dichroic Filter.

utilizes an unconventional focal-plane instrumentation (Fig. 1c), wherein a dichroic filter is sandwiched between the two detector arrays. The filter preferentially reflects wavelengths  $\lambda \sim 300\text{-}450$  nm from a Cerenkov event into the lower array of 16 'Blue'-sensitive detectors (B-channels) and transmits  $\lambda \sim 450\text{-}600$  nm into the upper array of 16 'Green'-sensitive detectors (G-channels). An LT-trigger is generated from the 3 VE by demanding a prompt coincidence between a B-pixel and the corresponding G-pixel, each operated at an unusually low single-channel discrimination level of  $\sim 4\text{pe}$  &  $8\text{pe}$  (corresponding to a single channel rate of  $\sim 10\text{MHz}$  in B- & G-pixels) and by concurrently applying the spectral cut  $N_B/N_G \geq 1.05$ , where  $N_B$  and  $N_G$  represent the numbers of photoelectrons registered in the B- and G-pixels respectively. This value is consistent with the spectrum of Cerenkov event detected in presence of the light of night sky (LONS) background. Residual noise-generated triggers can be effectively suppressed by demanding an appropriately delayed 3-fold coincidence among the outputs of the 3 VE (Tickoo et al., 1994).

At present, the Imaging Element is operational with an 81-pixel ( $9 \times 9$ ) camera and a 3NCT trigger-generator involving the innermost 36 pixels ( $9 \times 4$  configuration). In the present communication, we compare the trigger-thresholds of the IE and the VE and the effective collection areas of the IE with its two, above-referred trigger-generator configurations :

## 2. TACTIC simulations

Present simulation studies are based on the CORSIKA air-shower simulation code (Version 4.50; Knapp & Heck, 1995). In order to be compatible with the TACTIC geometry, the simulations are carried out after folding in a rectangular detector matrix, with each matrix element of  $4\text{m} \times 4\text{m}$  in area with an inter-element spacing of 6m along one axis and 10m along the other axis (Bhat, 1996). The principal axis of a TACTIC element is assumed to be directed towards the zenith angle  $\theta = 20^\circ$  and the primary  $\gamma$ -ray is assumed to be incident along the axis. Cosmic-ray proton directions, on the other hand, are selected randomly from within the effective telescope field of view (FOV), centred on  $\theta = 20^\circ$ . The basic database comprises the photon bunch size and its spatial coordinates in the observation plane, production height, direction cosines and arrival time at the detector. To keep the database size within manageable limits, sampling is done over the restricted wavelength interval  $\lambda = 300\text{-}320\text{nm}$ . Subsequently, a backup software generates all the Cerenkov photons which are likely to be received by a detector element over the broad wavelength region  $\lambda = 200\text{-}650\text{nm}$ , after duly accounting for the atmospheric attenuation. The photons, thus registered, are ray-traced to the detector focal-plane and the number of photoelectrons likely to be registered in a PMT pixel (ETL 9083 UVA for IE and ETL 9945B for VE) are inferred after folding in the relevant optical characteristics of the mirrors (reflection coefficient  $\sim 80\%$ ; see Udupa et al., 1993), the intervening dichroic filters (in case of VE's;  $\sim 90\%$  reflectivity,  $\lambda = 300\text{-}450$  nm;  $90\%$  transmission  $\lambda = 450\text{-}600$  nm), the metallic compound-paraboloid light concentrator at the entrance port of the pixels ( $\sim 75\%$  collection efficiency) and the photocathode spectral response. An appropriate amount of light of night-sky (LONS) noise is also injected into each pixel, based on the mean number of background photoelectrons ( $1\text{pe}$  &  $6\text{pe}$  for the IE and  $2\text{pe}$  &  $5\text{pe}$  for the B- and G-camera pixels respectively of the VE; e.g., Punch, 1994), likely to be seen by it and modulated as per the Poissonian statistics.

### 3. Results

The effective collection area of the IE has been derived using the 3NCT trigger-generation efficiency profile obtained for gamma ( $\gamma$ )- and proton (p)-events as a function of the shower core distance (Sapru et al., 1997). The results are shown in Fig. 2a, separately for  $\gamma$ - and p-events and for  $15 \times 15$  and  $4 \times 9$  pixel trigger-generators. It is evident that, for both event types, compared with the  $15 \times 15$  trigger-generator, the  $4 \times 9$  pixel version underestimates the effective Cerenkov light collection area by a factor of  $\sim 2$  at a primary energy  $> 1$  TeV. This is obviously because of too restricted FOV of the  $4 \times 9$  pixel configuration in one-dimension ( $\sim 1.2^\circ \times 2.8^\circ$ ). Fig. 2b shows the differential event rate as a function of the primary energy. Defined as the energy where the differential rate peaks, the  $\gamma$ -ray trigger-

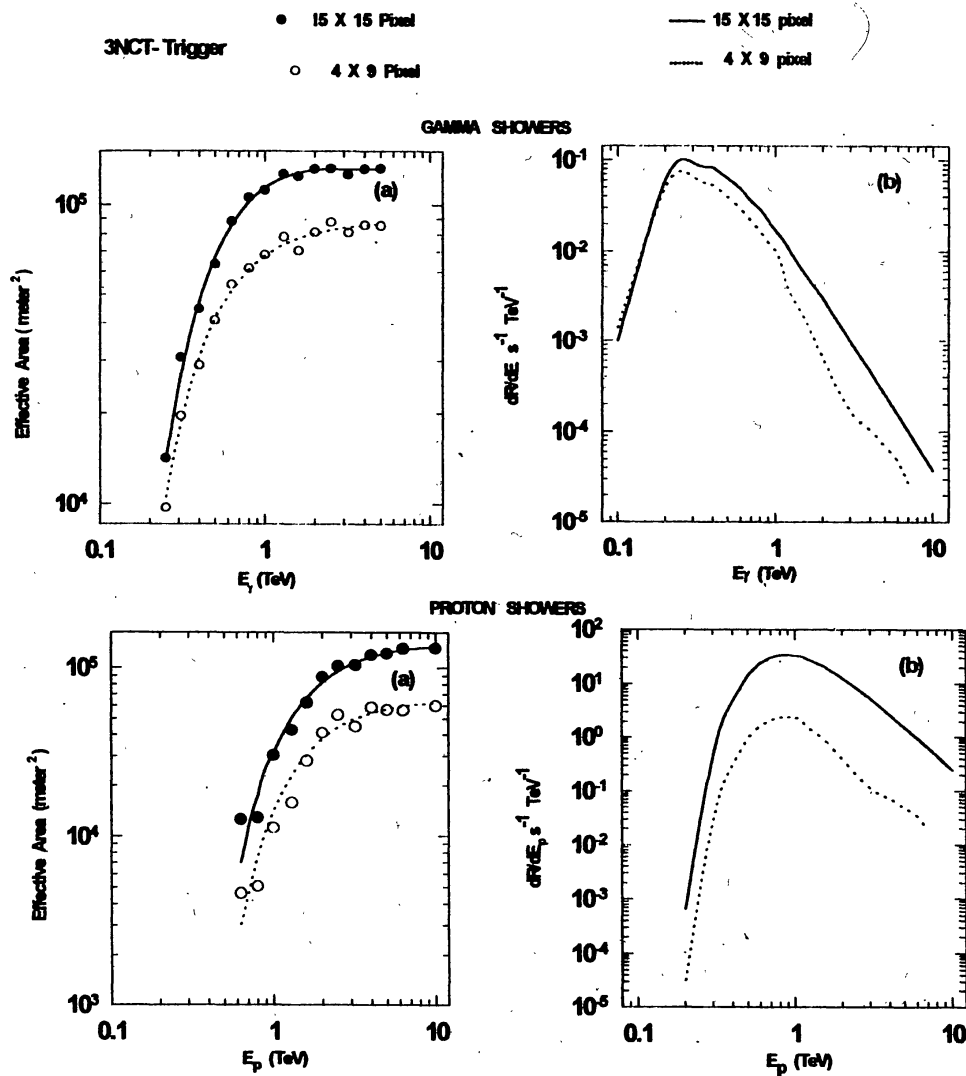
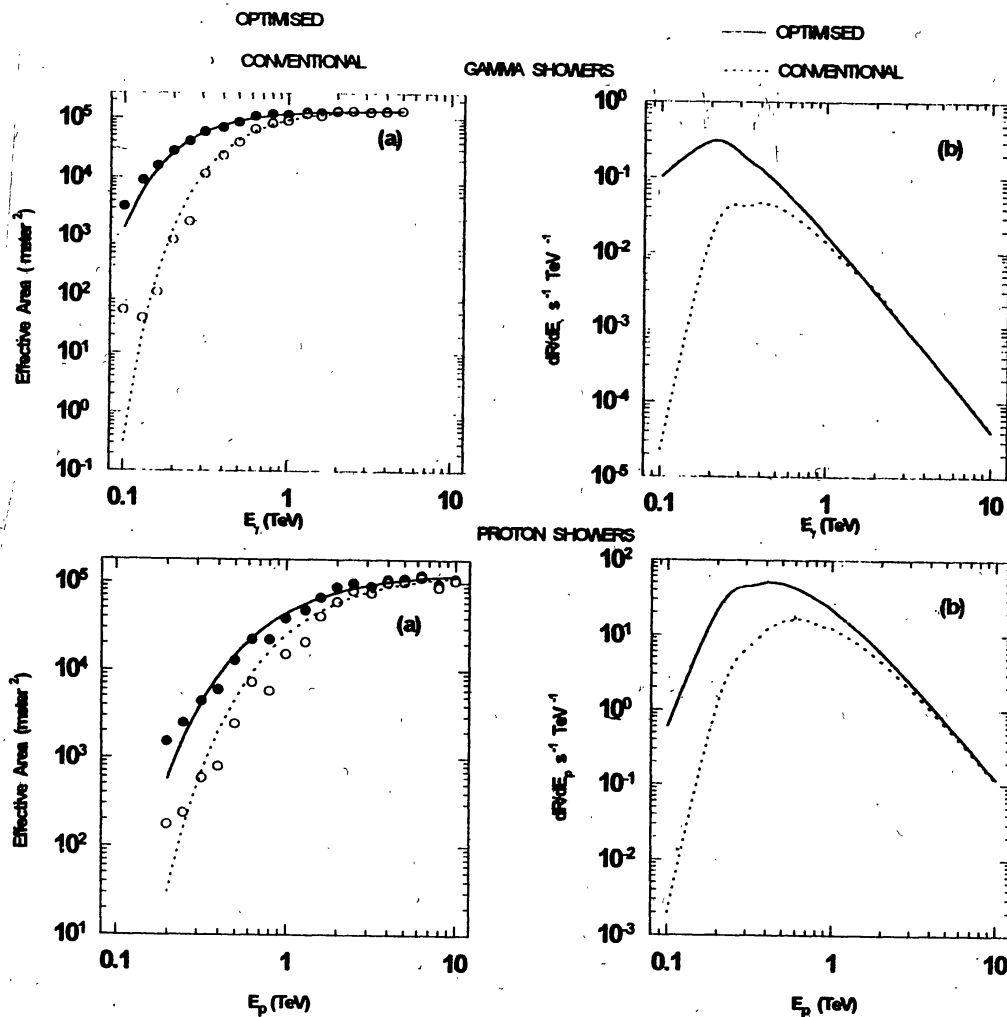


Figure 2. (a) Effective collection area of Imaging Element for the  $4 \times 9$  pixel (present) and  $15 \times 15$  pixel (final) trigger-generators, (b) Differential rates for IE indicating trigger-threshold energies for  $\gamma$ -ray and proton events.

threshold energy for both the trigger generators turns out to be  $\sim 0.3$  TeV, to be compared with  $\sim 1$  TeV for the proton events. The  $\gamma$ -rays source spectrum is assumed to be like that given recently by Lewis et al. (1993) for the Crab Nebular differential exponent  $\gamma_d = -2.7$  (same as that for cosmic-ray proton spectrum).

Fig. 3 provides a comparison of the efficiency of the LT trigger mode of operation for the VE with the conventional case where a single PMT detector is employed in the VE focal-plane. As seen in Fig. 3a, while the LT mode of operation provides almost the same effective collection area above 1 TeV primary energy as the conventional trigger mode, the effective area is significantly larger for the LT mode at lower primary energies for both  $\gamma$  and p-events. More importantly, as seen from Fig. 3b, the LT mode provides a significantly lower detection



**Figure 3.** (a) Effective collection area of Vertex Elements as a function of primary energy for Low-Threshold (open circles) and Conventional (filled circles) trigger-cuts, (b) Differential rates for Vertex Elements showing the trigger threshold for  $\gamma$ -ray and proton events.

threshold energy of  $\sim 0.2$  TeV and  $\sim 0.4$  TeV for the  $\gamma$ - and proton primaries respectively, to be compared with  $\sim 0.4$  TeV ( $\gamma$ -rays) and  $\sim 0.6$  TeV (protons for the conventional Cerenkov telescopes). This mode of operation is likely to be useful in observing sources which are particularly active in the sub-TeV range, like pulsars and active galactic nuclei.

#### 4. Conclusions

The results presented here suggest a reassuringly low  $\gamma$ -ray trigger-threshold energies for the IE ( $\sim 0.3$  TeV) and the VE ( $\sim 0.2$  TeV) and establish the superiority of the two innovative trigger-generation schemes being tried out for the first time on the TACTIC. We expect the  $\gamma$ -ray image (effective) threshold for the IE to be at least a factor of  $\sim 2$  higher, i.e.,  $\geq 0.6$  TeV.

#### References

- Bhat C. L. et al., 1994, NIM, A340, 413.  
Bhat C. L. et al., 1995, Proc. 24th ICRC, Rome, 3, 404.  
Bhat C. L. et al., 1996, Proc. Int. Colloquium "Perspectives in High Energy Astronomy and Astrophysics", Mumbai, pp 394.  
Knapp J., Heck D., 1995, Extensive Air Shower Simulation with CORSIKA : A User's Guide (Version 4.50).  
Lewis D. A. et al., 1993, Proc. "Int. Cosmic Ray Conf.", 1, 279.  
Punch M., 1994, Proc. "Towards a Major Atmospheric Cerenkov Detector-III", Kyoto, pp 163.  
Sapru M. L. et al., 1997, Proc. Workshop "Towards a Major Atmospheric Cerenkov Detector-V", Kruger Park, South Africa, pp 229.  
Tickoo A. K. et al., 1994, NIM, A349, 600.  
Udupa D. V. et al., Bull. Astron. Soc. India, 1993, 21, 527.  
Vishwanath P. R., 1996, Proc. Int. Colloquium "Perspectives in High Energy Astronomy and Astrophysics", Mumbai, pp 204.